J. Inst. Eng. India Ser. E (June 2022) 103(1):111–116
https://doi.org/10.1007/s40034-020-00194-x

ORIGINAL CONTRIBUTION

Nanoindentation and Morphological Studies on Polypropylene/Multi-wall Carbon Nanotubes Composite Fibers

B. Safaie[1] · **M. Youssefi**[1]

Received: 1 September 2020 / Accepted: 9 November 2020 / Published online: 24 November 2020

Abstract Nanoindentation technique was used to investigate the mechanical properties of polypropylene/multi-wall carbon nanotubes (MWCNT) nanocomposite fibers. The hardness and elastic modulus of the nanocomposite fibers were evaluated as a function of MWCNT concentration. It was found that incorporation of MWCNT enhanced the hardness and elastic modulus of the fibers. The elastic modulus data calculated from indentation load–displacement experiments were comparable with those obtained from tensile tests. DSC results also confirmed the increase in crystallinity of the polypropylene fibers due to the addition of MWCNT. The studies indicated that nanoindentation was a simple but efficient test method for evaluating the mechanical properties of nanocomposite fibers.

Keywords Nanoindentation · Polypropylene · Carbon nanotube · Fiber · Nanocomposite

Introduction

Carbon nanotubes (CNT) have received extensive attention in recent years due to such considerable properties as high modulus, electrical/thermal conductivity and tensile strength as high as 200 GPa [1]. Extremely strong materials could be obtained by combining a polymer matrix with CNTs [2–5]. In several research works, single-wall (SWCNT) and multi-wall (MWCNT) carbon nanotubes have been used to enhance the mechanical, thermal and electrical properties of neat fibers [6–11]. Composite materials are used in a variety of applications such as sporting goods, electronic appliances and where high stiffness and light weight are required. The correlation between the structure of materials and their properties in composite materials is an important subject from both the academic and industrial points of view [12–14]. In industrial applications, for example tire cords or ropes, are needed high strength and modulus. The cost of textile fibers is usually below 5 $/kg, while the cost of high-performance fibers is above 40 $/kg. There is a significant price gap between textile fibers (such as PET, nylon, polypropylene) and high-performance fibers (such as Kevlar and Zylon). The preparation of a carbon nanotube/polymer composite makes it possible to reduce the gap between these two classes of fibers [15]. The properties of the nanocomposite fibers are not only influenced by the kind of fillers, but also by the microstructure of the polymer and the preparation process. Dispersion and orientation of CNT in the polymer matrix are the necessary factors to achieve optimum property improvements. The CNTs can be dispersed in the polymer matrix using several techniques such as melt processing, solution processing or in situ polymerization [16–20]. There are some papers which have discussed the structure and properties of polypropylene/CNT fibers. For example, Choi et al. [4] and Yetgin [11] examined the thermal and mechanical properties of polypropylene filaments reinforced with MWNTs. Kearns et al. [6] studied the tensile properties of composite fibers of polypropylene/SWCNT. Jose et al. [7] studied the aligning of CNTs in those polypropylene fibers produced by melt spinning.

To our knowledge, although the mechanical properties of PP/MWCNT fibers have been investigated before, the local mechanical and indentation properties of these fibers have not been widely investigated yet. In this study,

✉ M. Youssefi
youssefi@cc.iut.ac.ir

[1] Department of Textile Engineering, Isfahan University of Technology, Isfahan 84156-83111, Iran

composite fibers of PP/MWCNT were produced with varying levels of MWCNTs using melt compounding and melt spinning processes. The structure, tensile properties and nanoindentation properties of the fibers were investigated.

Experimental

Materials

Fiber grade polypropylene homopolymer (PP) with a melt flow rate of 16 g/10 min (230 °C/2.16 kg) was obtained from Tabriz Petrochemical Co. (Tabriz, Iran). Multi-walled carbon nanotubes (MWCNT) with the purity of $> 95\%$, the diameter of 10–30 nm and the average length of 10 μm were supplied from petroleum research laboratory of Iran.

Methods

The PP/MWCNT nanocomposites containing 0.25, 0.50, 1 wt% MWCNT were melt-compounded using a twin screw extruder (Brabender model 2000) at temperatures in the range of 180–190 °C and a screw speed of 105 rpm. A sample of polypropylene was prepared under the same conditions without adding MWCNT as a reference sample. Fibers containing 0% (PP), 0.25 wt% (PP0.25), 0.5 wt% (PP0.5) and 1 wt% (PP1) of MWCNT were produced by a melt spinning apparatus (Fourne Bonne Melt Spinner, Germany) and drawn using a Zinser drawing machine up to the draw ratio of 3. Longitudinal view of the composite fibers was examined by a field emission electron microscope (FE-SEM Hitachi S-4160, Japan) operating at 30 kV. An automatic sputter coater was used to coat the fibers with gold before examination by FE-SEM. Tensile properties of the samples were measured at room temperature with a constant rate of elongation tester (Zwick 1446-60, Germany). The gauge length was 10 cm, and the crosshead speed was 7 cm/min. After at least 30 measurements on each sample, the average and 95% confidence limits were calculated. Indentation experiments were performed using an NHTX-S nanoindenter with a continuous stiffness measurement technique. The indenter was diamond three-sided pyramidal Berkovich tip with a face angle of 65.3°. Approach speed of indenter was 1500 nm/min. A loading rate of 60 mN/min was maintained constant during the increment of the load until the maximum load of 30 mN was reached. The load was then held constant for 10 s to prevent the creep. The indenter was then withdrawn from the surface at the same rate. Differential scanning calorimetry characterization (DSC 2910, TA Instruments) was performed to investigate crystallization and melting behaviors of the composite fibers. Samples with the same weight (4.5 mg) were heated from 20 to 230 °C at a heating rate of 10 °C/min under a nitrogen atmosphere. The crystallinity (x) for unfilled PP and composite fibers was calculated according to the DSC data from the heating scan [21]. Thermo-gravimetric analysis of the samples was carried out using the Mettler Toledo TGA/STA 851. Samples were heated at the rate of 20 °C per minute from 50 to 900 °C under a nitrogen atmosphere.

Results and Discussion

Figure 1 shows FE-SEM images of the samples. As shown in the figure, the morphology and the cracks on the surface of the fibers were not changed due to the addition of MWCNT. At the surface of composite fibers, some of the nanotubes were observed. There was also no sign of aggregation of the MWCNT as revealed in these images.

As seen in Fig. 2, breaking stress and modulus of the samples were increased with the increase in MWCNT concentration. The highest breaking stress was observed for the PP1 sample and the highest modulus was observed for the PP0.5 sample. It was expected that adding small amounts of nanotubes to matrix improved the mechanical properties up to an optimal concentration and above which nanotube aggregation could result in fiber strength decrease via stress concentrations. The effect of carbon nanotube aggregation on mechanical properties has been reported in several studies [16, 22, 23]. According to Gorga and Cohen [22], the mechanism for the improvement in mechanical properties is based on bridging of CNT between crazes and cracks formed during the tensile test. The CNTs bridge between the gaps formed by the cracks (shown schematically in Fig. 3); therefore, they decelerate the crack propagation and increase the material toughness. Dondero and Gorga [16] stated that in semi-crystalline materials, such as PP, the nanotubes acted as tie molecules between crystalline regions rather than crack bridges, thereby also acting as tougheners. The increase in modulus can be attributed to load transfer (from the matrix to nanotube) or crystallinity changes in composite due to the addition of MWNTs. The effects of MWCNT on the crystal structure of composite fibers were studied in our previous work [24]. Nanotubes aggregation results in the decrease in mechanical properties, forming stress concentrations like those caused by voids in composite systems [16, 25]. Besides, in the fiber spinning process, high applied stress during spinning and drawing can result in the orientation of the crystallites inside the fiber; the consequence is a high-strength fiber. Since nanotubes are of comparable size to the crystallites, the nanotubes will most likely orient in a manner similar to the crystallites [17, 26]. One point which must be considered is that the obtained breaking strength

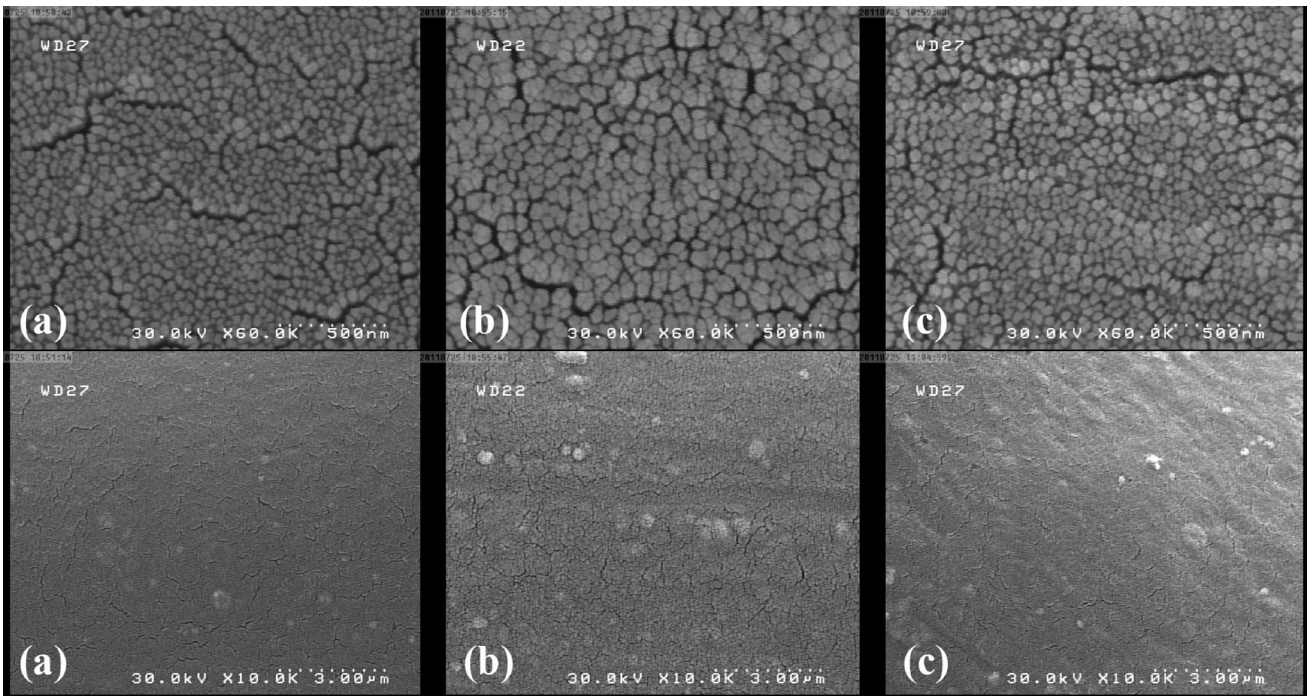

Fig. 1. The FE-SEM images of the samples, (**a**) PP, (**b**) PP1, (**c**) PP0.5

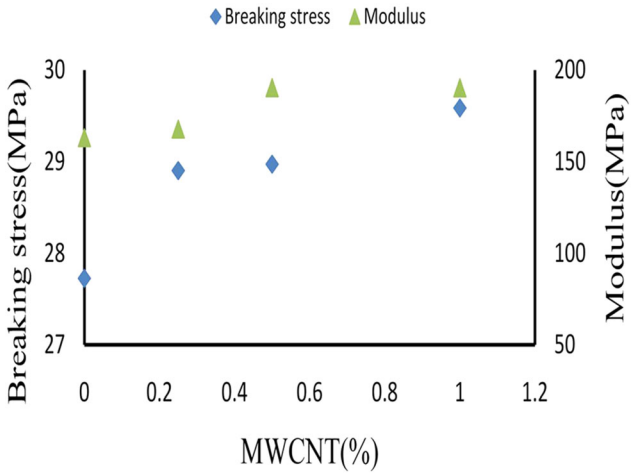

Fig. 2. Breaking stress and modulus versus MWCNT loading

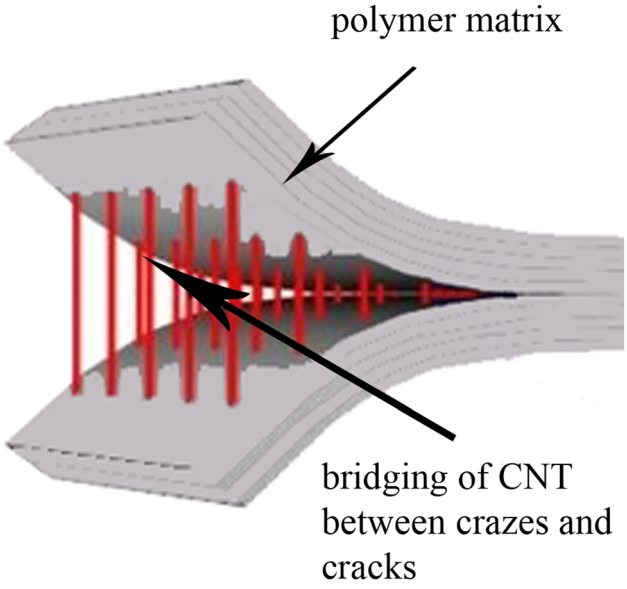

Fig. 3. Schematic diagram of CNT bridging between cracks in the composite

for the composite fibers was far lower than the theoretical expectation; e.g., according to the rule of mixture for PP1 sample, the theoretical value for composite modulus is 4.9 GPa [27]. Therefore, it may be said that poor adhesion of the CNT to the matrix, imperfections and defects in the nanotube structure and the insignificant dispersion of nanotube within matrix resulted in a reduced composite modulus [6]. If the revised models are used instead of simple mixing model, the mechanical properties of the composite fibers can be predicted more accurately [28–30].

In an indentation test, the hardness is defined as the indentation load divided by the projected contact area, as shown in Eq. 1.

$$H = \frac{F_{\max}}{A} \tag{1}$$

A is the contact area between the sample surface and the indenter at the maximum load ($F_{\max}$). The elastic modulus

of the sample can be calculated based on relationships illustrated in Eq. 2 [31]. Upon loading, the forces are incremented at constant velocities.

$$S = \frac{\mathrm{d}f}{\mathrm{d}h} = 2\beta\sqrt{\frac{A}{\pi}}E_{\mathrm{r}} \tag{2}$$

where S is the contact stiffness of the sample and h is the penetration depth. β is a constant depending on the geometry of the indenter; for indenter type of Berkovich, it is 1.034. E_{r} is the reduced elastic modulus, as obtained from Eq. 3.

$$\frac{1}{E_{\mathrm{r}}} = \frac{1-v^2}{E} + \frac{1-v_{\mathrm{i}}^2}{E_{\mathrm{i}}} \tag{3}$$

E_{r}, E and E_{i} are the reduced elastic modulus, modulus of the sample and elastic modulus of the diamond indenter, respectively. v and v_{i} are Poisson's ratio of the sample and the diamond indenter. In reference**,** elastic modulus and Poisson's ratio of the diamond indenter are 1141 GPa and 0.07, respectively [31, 32].

As can be seen in Fig. 4, the curves were steadily shifted left side with increasing MWCNT content, indicating that the nanocomposites' resistance to indentation was gradually increased with MWCNT concentration. That is to say, the addition of nanotubes to the matrix decreased penetration depth and as a consequence increased the samples hardness. The softer material surface required lower normal loads to induce a comparable indenter penetration. Therefore, the results indicated that MWCNT addition enhanced the hardness of the fibers with increasing MWCNT content. Figure 5 shows the fibers hardness as a function of penetration depth. It was observed that for all of the samples, the hardness of both fibers was decreased with the increase in penetration depth. According to references [31, 33–35], the apparent decrease of modulus and

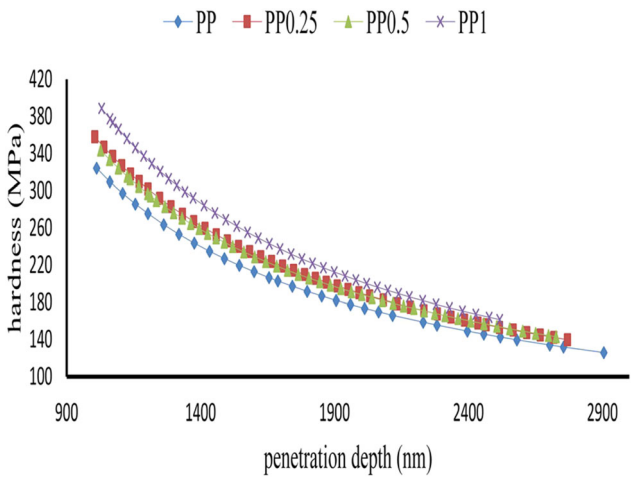

Fig. 5. Hardness versus penetration depth

hardness at deeper depth was widely observed in most polymeric systems. It could be attributed to indentation size effects such as a non-negligible tip defect or imperfection of the indenter used, an intrinsic 'blunting effect' of the indenter tip or other experimental errors such as surface roughness or imprecise location of the point of initial contact.

The mechanical properties of the samples obtained by tensile tests and nanoindentation measurements are illustrated in Fig. 6. It was observed that hardness and modulus of the fibers were steadily increased with increasing nanotube concentration (up to 0.5%), indicating the reinforcement effect of well-dispersed nanotube within the matrix [31]. The modulus values obtained from indentation measurements had concordance with the results of tensile tests. There were some differences between the results of indentation experiments and tensile measurements which seemed to be due to the difference in loading direction; in

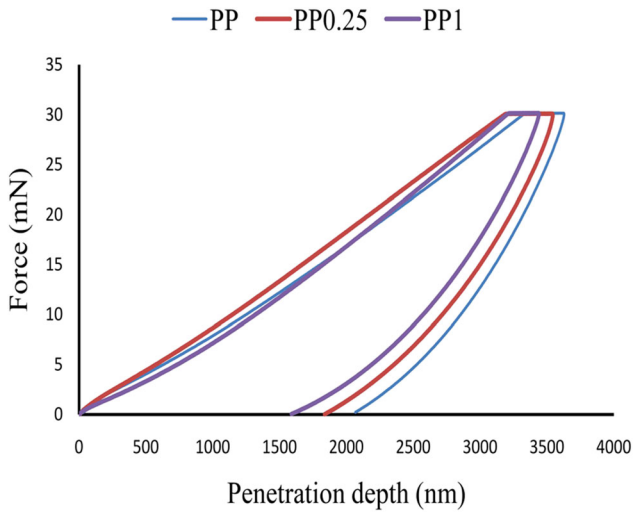

Fig. 4. The load-penetration depth curves

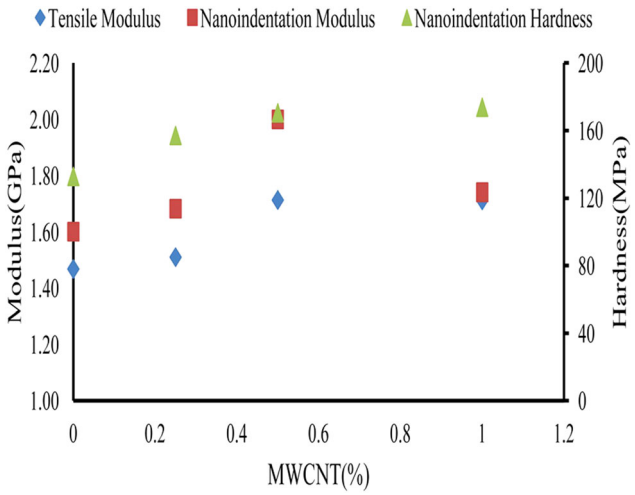

Fig. 6. Hardness and modulus versus MWCNT loading

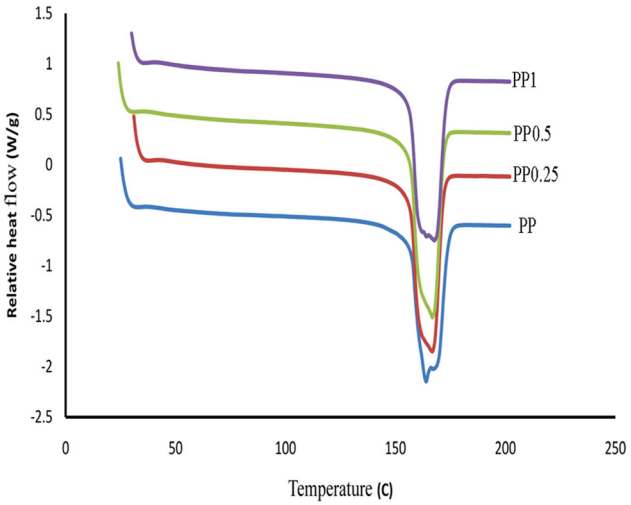

Fig. 7. The DSC thermograms of the composite fibers

Table 1 The data obtained from the DSC measurements

	PP	PP0.25	PP0.5	PP1
Melting heat (J/g)	124.0	126.4	133.7	127.1
Melting temperature (°C)	163.5	166.6	166.8	167.7
Crystallinity (%)	59.3	60.6	64.3	61.4

tensile testing, the direction of the applied force was in draw axis direction, but in nanoindentation testing, the compressive force direction was perpendicular to the drawing axis. The modulus values for a sample of 1% nanotube had lower values as compared to PP0.5; the probable explanation for this phenomenon is this point that in PP1 sample, some aggregation of nanotubes occurred.

The DSC thermographs of the samples are shown in Fig. 7. The melting heat, melting temperature, and degree of crystallinity of the fibers were obtained from the thermographs, as summarized in Table 1. The main stable crystalline form of PP was the α-form, which had a monoclinic structure and was obtained from melted PP without any special treatment [7]. The melting temperature range of α-PP was 160–165 °C, similar to the melting temperature obtained in our study. This suggests that the pure PP and the composite fibers were in the stable α-crystalline form. Crystallinity can have a major effect on the mechanical properties of polymers; that's why the effect of nanoparticles on nucleation and crystallinity development is of interest. The melting heat obtained was used to calculate the crystallinity percentage of the samples. As the MWNTs concentration was increased, the crystallinity percentage and melting temperature of the samples were increased. The increase in the ΔH_f with increasing MWCNT concentration could be attributed to the proportional increment of the nucleation of the PP crystallites, which were induced by the nanotubes [23, 36].

As shown in the TGA plots of the samples in Fig. 8, no significant weight loss was observed until 400 °C, and then, degradation was continued up to 500 °C. However, the onset of degradation temperature was higher for the samples containing higher amounts of MWNT. This indicated that the addition of MWNT improved the decomposition stability of the PP matrix in nanocomposite fiber. The improvement in thermal stability in the samples due to the addition of MWCNT can be attributed to good matrix–nanotube interaction and also the thermal conductivity of the nanotubes. The appropriate dispersion of nanotubes in

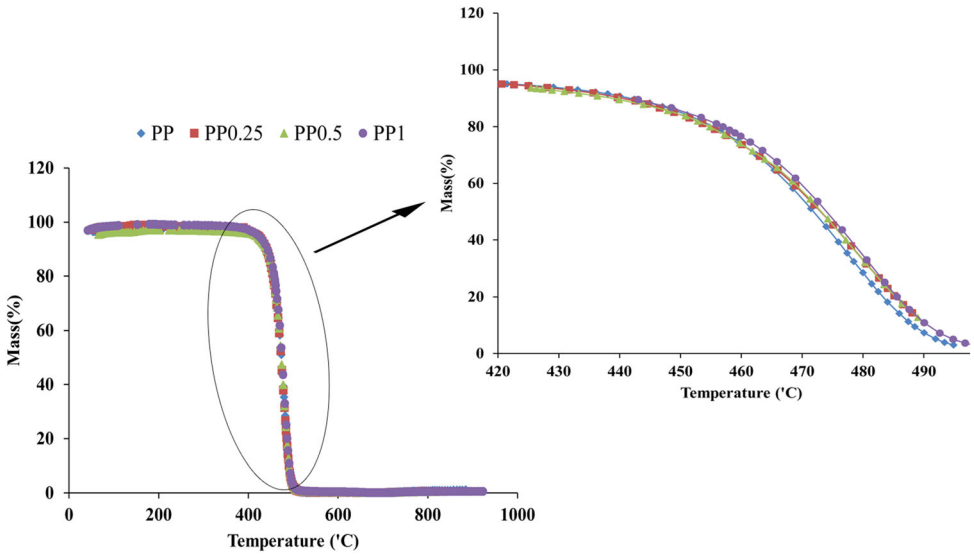

Fig. 8. The TGA curves of the composite fibers

the polymer matrix allowed the spreading of heat uniformly along the fiber. According to Kim et al. [36], another factor that can potentially contribute to the thermal stability is the formation of a comparatively even network-structured layer which covers the whole sample surface without any cracks or gaps formed during heating. This layer re-emits much of the incident radiation back from its hot surface, thus reducing the heat transmitted to the PP layers underneath. This improved thermal stability is dependent on the size and shape and the amount of filler particles. Besides, TGA measurements showed that thermal stability of the fibers was improved slightly due to the addition of MWCNT.

Conclusion

Composite fibers of PP/MWCNT with varying amounts of MWCNT (up to 1%) were produced, and the effect of MWCNT addition on the hardness, tensile properties and morphology of polypropylene/MWCNT nanocomposites were investigated as a function of MWCNT loading. It was shown that the hardness and the elastic modulus were gradually enhanced with increasing MWCNT concentration. The elastic modulus obtained by nanoindentation was comparable with those obtained from tensile tests. Therefore, the addition of small amounts of MWCNT resulted in increasing the hardness of the composite fibers. This was likely due to the increase in crystallinity of the fibers. The DSC results also confirmed this conclusion, indicating that the crystallinity of the composite fibers was increased due to the nucleation effect of nanotubes. In both test methods (nanoindentation and tensile tests), the modulus of the fibers containing 1% MWCNT was lower than that of fibers containing 0.5% MWCNT. This could be attributed to some probable aggregation of MWCNT in the fibers containing 1% MWCNT. CNT composite fibers are used in variety of applications such as sensors, anti-static, electromagnetic interference shield, filters, smart clothing of protection for dust and germ, ropes and tire cords.

References

1. J.E. Fischer, in *Carbon nanotubes: structure and properties*, ed. by Y. Gogotsi (Taylor and Francis Group, New York, 2006), pp. 41–76
2. H. Djoudi, J.C. Gelin, T. Barriere, Int. J. Adv. Manuf. Technol. **83**, 1659 (2016)
3. P. Wang, P. Gulgunje, S. Ghoshal, N. Verghese, S. Kumar, Polym. Eng. Sci. **59**(9), 1763 (2019)
4. S. Choi, Y. Jeong, G. Lee, D. Cho, Fibers Polym. **10**(4), 513 (2009)
5. A. Zadhoush, R. Reyhani, M. Naeimirad, Polym. Compos. (2018). https://doi.org/10.1002/pc.24799
6. J. Kearns, R. Shambaugh, J. Appl. Polym. Sci. **86**(8), 2079 (2002)
7. M. Jose, D. Dean, J. Tyner, G. Price, E. Nyairo, J. Appl. Polym. Sci. **103**(6), 2844 (2007)
8. I. Mazov, I. Burmistrov, I. Il'inykh, A. Stepashkin, D. Kuznetsov, J. Issi, Polym. Compos. **36**(11), 1951 (2015)
9. M.H. Al-Saleh, Mater. Des. **85**, 76 (2015)
10. S. Gong, Z. Zhu, S. Meguid, Polymer **56**, 498 (2015)
11. S.H. Yetgin, J. Mater. Res. Technol. **8**(5), 4725 (2019)
12. Y. Ma, D. Wu, Y. Liu, X. Li, H. Qiao, Z. Yu, Compos. B **56**, 384 (2014)
13. M. Hong, W. Choi, K. An, S. Kang, S. Park, Y. Lee, J. Ind. Eng. Chem. **20**(5), 3901 (2014)
14. B. Coppola, L. Di Maio, L. Incarnato, J. Tulliani, Nanomaterials **10**(4), 814 (2020)
15. B.G. Min, H.G. Chae, M.L. Minus, S. Kumar, Funct. Compos. Carbon Nanotubes Appl. **2**, 43 (2009)
16. W. Dondero, R. Gorga, J. Polym. Sci. Part B Polym. Phys. **44**(5), 864 (2006)
17. J. Zhong, A. Isayev, Polym. Compos. (2015). https://doi.org/10.1002/pc.23867
18. S. Tastani, M. Konsta-Gdoutos, S. Pantazopoulou, V. Balopoulos, Front. Struct. Civ. Eng. **10**(2), 214 (2016)
19. P. Boonruksa, D. Bello, J. Zhang, J. Isaacs, J. Mead, S. Woskie, Ann. Occup. Hyg. **60**(1), 40 (2016)
20. B. Lee, J. Cho, K.H. Kim, Eur. Polym. J. **91**(Supplement C), 70 (2017)
21. T. Soitong, J. Pumchusak, J. Mater. Sci. **46**(6), 1697 (2011)
22. R.E. Gorga, R.E. Cohen, J. Polym. Sci. B Polym. Phys. **42**(14), 2690 (2004)
23. D. Xu, Z. Wang, Polymer **49**(1), 330 (2008)
24. M. Youssefi, B. Safaie, Fibers Polym. **14**(10), 1602 (2013)
25. M. Youssefi, B. Safaie, J. Inst. Eng. India Ser. E. (2018). https://doi.org/10.1007/s40034-017-0110-3
26. G. Wu, Q. Li, J. Cuculo, Polymer **41**(22), 8139 (2000)
27. M. Yu, O. Lourie, M. Dyer, K. Moloni, T. Kelly, R. Ruoff, Science **287**(5453), 637 (2000)
28. J.N. Coleman, M. Cadek, R. Blake, V. Nicolosi, K.P. Ryan, C. Belton, A. Fonseca, J.B. Nagy, Y.K. Gunko, W.J. Blau, Adv. Funct. Mater. **14**(8), 791 (2004)
29. S. Kanagaraj, F.R. Varanda, T.V. Zhiltsova, M.S. Oliveira, J.A. Simoes, Compos. Sci. Technol. **67**, 3071 (2007)
30. V. Mittal, *Optimization of Polymer Nanocomposite Properties* (Wiley, London, 2009)
31. Y. Hu, L. Shen, H. Yang, M. Wang, T. Liu, T. Liang, Polym. Test. **25**(4), 492 (2006)
32. W. Oliver, G. Pharr, J. Mater. Res. **7**(06), 1564 (1992)
33. L. Shen, I. Phang, L. Chen, T. Liu, K. Zeng, Polymer **45**(10), 3341 (2004)
34. R. Lesan-Khosh, R. Bagheri, S. Asgari, J. Appl. Polym. **121**(2), 930 (2011)
35. W. Nix, H. Gao, J. Mech. Phys. Solids. **46**(3), 411 (1998)
36. J. Kim, Y. Jung, Y. Kwark, Y. Jeong, J. Appl. Polym. **118**(3), 1335 (2010)